Membrane and Water Treatment, *Vol. 13, No. 4 (2022) 167-172*
https://doi.org/10.12989/mwt.2022.13.4.167

Mass transfer in the filtration membrane covering from macroscale, multiscale to nanoscale

Wei Lin[1,2], Jian Li[2] and Yongbin Zhang[*2]

[1]*School of Mechanics Technology, Wuxi Institute of Technology, Wuxi, Jiangsu Province, China*
[2]*College of Mechanical Engineering, Changzhou University, Changzhou, Jiangsu Province, China*

(Received March 13, 2021, Revised May 9, 2022, Accepted May 15, 2022)

Abstract. The analytical results are presented for the mass transfer in a cylindrical pore covering from the macroscale, multiscale to nanoscale owing to the variation of the inner diameter of the pore. When the thickness h_{bf} of the physically adsorbed layer potentially fully formed on the pore wall is comparable to but less than the inner radius R_0 of the pore, the multiscale flow occurs consisting of both the nanoscale non-continuum adsorbed layer flow and the macroscopic continuum liquid flow; When $R_0 \leq h_{bf}$, the flow in the whole pore is essentially non-continuum; When R_0 is far greater than h_{bf}, the flow in the whole pore can be considered as macroscopic and continuum and the adsorbed layer effect is negligible.
Keywords: cylindrical pore; mass transfer; multiscale; non-continuum

1. Introduction

The size of the filtration pore of the membrane can be varied widely depending on the filtered media. In conventional filtration membranes, the radius of the filtration pore is usually far larger than the size of the molecule of the flowing liquid, and the flow is on the macroscale and can be modeled by continuum hydro-dynamic theories (Yang *et al*. 2012, Yoon 2018, Wang *et al*. 2013). In nanoporous filtration membranes, the radius of the filtration pore is on the 1nm or 10nm scales, often comparable to the molecule size of the flowing liquid, for realizing the super purification (Bottino *et al*. 2011, Brown *et al*. 1975, Elizabeth *et al*. 2012, Sanjay *et al*. 2021). In the applications of nanoporous filtration membranes such as for ultimate purification, hemofiltration and DNA analysis, the filtration pore is so small that it can only contain several molecule layers of the flowing media, and the flow inside the filtration pore is essentially on the nanoscale with the non-continuum behavior (Fissel *et al*. 2009, Jackson and Hillmyer 2010, Surwade *et al*. 2015). In the liquid-particle separation, because of the size of the filtered particle, the radius of the filtration pore can also be significantly bigger so that the thickness of the physically adsorbed layer potentially fully formed on the pore wall is comparable to but less than the inner radius of the filtration pore; In this case, inside the filtration pore actually occurs the multiscale flow consisting of both the nanoscale non-continuum adsorbed layer flow and the macroscopic continuum liquid flow (Atkas and Aluru 2002, Borg *et al*. 2013). Although the experimental studies on microporous or nanoporous filtration membranes have been carried out a lot (Ariono *et al*. 2018, Baker and Bird 2008, El-ghzizel *et al*. 2019, Jin *et al*. 2019), the theoretical researches on the flow and mass transfer in these membranes are only a few regarding the multiscale and nanoscale flow regimes. Atkas and Aluru (2002) used molecular dynamics simulation (Monte Carlo Method) to model the non-continuum layer flow near the solid wall and used the Stokes equation to simulate the continuum liquid flow in the other area in the study of microporous membrane filtration. Their multiscale scheme will face the computational difficulty when simulating the relatively thick membrane because of the huge cost of the computational time and computer storage. Borg *et al*. (2018) also used this multiscale method to simulate the water flow through the filtration membrane with the diameter of the filtration pore below 2nm for a laboratory-scale membrane. Their multiscale scheme is usually not applicable for an engineering multiscale flow because of the implementation of the molecular dynamics simulation in the over large area. On the other hand, full molecular dynamics simulation is intractable for the flow in these membranes because of the too huge computational burden caused by the over large membrane size; It is often seen to simulate the flow in the biological membrane such as the cell membrane because of the small thicknesses of these membranes only on the scales of 1nm or 10nm (Khalili-Araghi *et al*. 2009).

For overcoming the computational difficulty, by using the newly derived closed-form explicit flow equations for the multiscale flow (Zhang 2020, 2021) and the formerly derived non-continuum nanoscale flow equation (Zhang 2016), both of which were shown to be ultra efficient for an engineering flow, the present paper aims to investigate the influences of both the liquid-pore wall interaction and the pore diameter on the mass transfer through the microporous or nanoporous filtration membranes in the wide range of the operational parameter values covering the macroscale, multiscale to nanoscale flows. The flow phenomena inside the mentioned filtration membranes are thus able to be more

*Corresponding author, Professor
E-mail: engmech1@sina.com

ISSN: 2005-8624 (Print), 2092-7037 (Online)

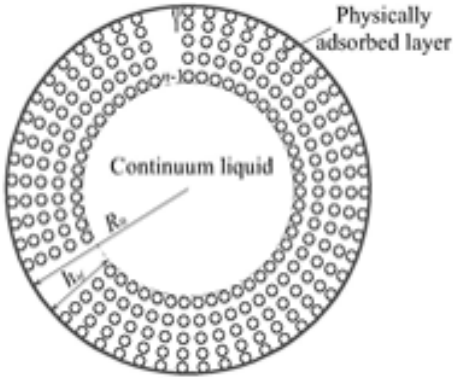

Fig. 1 Liquid flow in the filtration pore of microporous or nanoporous filtration membranes; The orientated molecule layers are formed on the pore wall because of the liquid physical adsorption to the pore wall

easily explored. The obtained results should be indicative to the design of the relevant filtration membranes in engineering use.

2. Flow equations for the different flow regimes in the membrane

Fig. 1 shows the filtration pore in a micro/nano porous filtration membrane inside which the flowing media is contained. Dependent on the inner radius R_0 of the filtration pore due to the filtration requirement, the thickness h_{bf} of the physically adsorbed layer potentially fully formed on the pore wall can be lower than but comparable to the magnitude of R_0, far lower than R_0, or greater than R_0. For these three cases, the flow regimes in the membrane are qualitatively different.

The physically adsorbed layer shown in Fig. 1 may be the equivalent layer. The actual adsorbed layer may not be exactly like as Fig.1 shows. The flow in the membrane is driven by the pressure difference. In the present study, the wall slippage is neglected, and the Poiseuille flow occurs inside the filtration pore. The inside wall of the pore is assumed as identical everywhere. The present analysis is thus not for the asymmetric filtration pore.

2.1 For the multiscale flow

When h_{bf} is lower than but comparable to R_0, in the filtration pore simultaneously occur the nanoscale non-continuum adsorbed layer flow and the macroscopic continuum liquid flow both of which may be significant. The analytical approach should solve these two flows by considering the boundary conditions and the two different flow regimes. According to the developed analysis (Zhang 2021), in this multiscale flow, the total mass flow rate through the pore is expressed as:

$$q_m = 2\pi R_{e,0}\left[\frac{F_1 h_{bf}^3}{12\eta_{bf,1}^{eff}}\frac{\partial p}{\partial x} - \frac{h_{bf}^3}{2\eta_{bf,1}^{eff}}\frac{\partial p}{\partial x}\left(1+\frac{1}{2\lambda_{bf,0}} - \frac{q_0-q_0^n}{q_0^{n-1}-q_0^n}\frac{\Delta_{n-2}}{h_{bf}}\right)\frac{\varepsilon}{1+\frac{\Delta x}{D}}\right]\rho_{bf,1}^{eff} + \left\{\frac{4}{\eta_{bf,1}^{eff}}\left[\frac{F_2\lambda_{bf,0}^2}{6} - \frac{\lambda_{bf,0}}{1+\frac{\Delta x}{D}}\left(\frac{1}{2}+\lambda_{bf,0} - \frac{(q_0-q_0^n)\Delta_{n-2}}{2(q_0^{n-1}-q_0^n)(R_0-h_{bf})}\right)\right] - \frac{1}{4\eta}\right\}\cdot\pi\rho(R_0-h_{bf})^4\frac{\partial p}{\partial x}, \quad \text{for } R_0 > h_{bf} \tag{1}$$

where p is the driving pressure, x is the coordinate in the pore axial direction, D is the diameter of the liquid molecule, $R_{e,0} = R_0\left(1-\frac{\lambda_x}{2}\right)$, $\lambda_{bf,0} = \frac{\lambda_x}{[2(1-\lambda_x)]}$, $\lambda_x = \frac{h_{bf}}{R_0}$, ρ and η are the bulk density and the bulk viscosity of the liquid flowing through the membrane respectively, $\rho_{bf,1}^{eff}$ and $\eta_{bf,1}^{eff}$ are the average density and the effective viscosity of the adsorbed layer across the layer thickness respectivel $\eta_{bf,1}^{eff} = Dh_{bf}/[(n-1)(D+\Delta_x)(\Delta_l/\eta_{line,l})_{avr,n-1}]$, $q_0 = \frac{\Delta_{j+1}}{\Delta_j}$ and q_0 is constant, Δx is the separation distance between the neighboring liquid molecules in the flow direction in the adsorbed layer, $\varepsilon = (2DI+II)/[h_{bf}(n-1)(\Delta_l/\eta_{line,l})_{avr,n-1}]$, $F_1 = \eta_{bf}^{eff}(12D^2\psi + 6D\phi)/h_{bf}^3$, and $F_2 = 6\eta_{bf}^{eff}D(n-1)(l\Delta_{l-1}/\eta_{line,l-1})_{avr,n-1}/h_{bf}^2$; Here, $I = \sum_{i=1}^{n-1} i(\Delta_l/\eta_{line,l})_{avr,i}$, $II = \sum_{i=0}^{n-2}[i(\Delta_l/\eta_{line,l})_{avr,i} + (i+1)(\Delta_l/\eta_{line,l})_{avr,i+1}]\Delta_i$, $\psi = \sum_{i=1}^{n-1} i(l\Delta_{l-1}/\eta_{line,l-1})_{avr,i}$, $\varphi = \sum_{i=0}^{n-2}[i(l\Delta_{l-1}/\eta_{line,l-1})_{avr,i} + (i+1)(l\Delta_{l-1}/\eta_{line,l-1})_{avr,i+1}]\Delta_i$, $i(\Delta_l/\eta_{line,l})_{avr,i} = \sum_{j=1}^{i}\Delta_{j-1}/\eta_{line,j-1}$, $i(l\Delta_{l-1}/\eta_{line,l-1})_{avr,i} = \sum_{j=1}^{i} j\Delta_{j-1}/\eta_{line,j-1}$, $\eta_{line,j-1}$ and Δ_{j-1} are the local viscosity and the local separation distance between the j^{th} and $(j-1)^{th}$ molecules (or molecule layers) across the adsorbed layer thickness respectively, j and $(j-1)$ are the order numbers of the molecules (or the molecule layers) across the adsorbed layer thickness respectively as shown in Fig. 1, and n is the number of the molecule layers across the adsorbed layer thickness.

2.2 For the nanoscale flow

When $R_0 \le h_{bf}$, the macroscopic continuum liquid disappears and only the nanoscale non-continuum adsorbed layer remains in the pore. For this case, the flow inside the whole pore is essentially non-continuum, and it is heavily influenced by the liquid-pore wall interaction. In this case, the mass flow rate through the pore is (Zhang 2016 and 2017):

$$q_m = \frac{\pi\rho_{bf,2}^{eff}(R_0)S(R_0)R_0^4}{4\eta_{bf,2}^{eff}(R_0)}\frac{\partial p}{\partial x}, \text{ for } R_0 \le h_{bf} \tag{2}$$

where $\rho_{bf,2}^{eff}$ and $\eta_{bf,2}^{eff}$ are the average density and the effective viscosity of the adsorbed layer across the pore radius respectively, and S $(-1 < S < 0)$ is the parameter accounting for the non-continuum effect of the adsorbed layer due to the discontinuity and inhomogeneity across the adsorbed layer thickness (Zhang 2016); Stronger the

liquid-pore wall interaction, smaller the absolute value of S and thus stronger the non-continuum effect of the adsorbed layer (Zhang 2016).

2.3 For the conventional macroscopic flow

When R_0 is far greater than h_{bf}, the adsorbed layer effect is negligible and the flow in the whole pore can be considered as macroscopic and continuum. For this case, the macroscopic flow theory can be applied, and the mass flow rate through the pore is:

$$q_{m,conv} = -\frac{\pi\rho R_0^4}{4\eta}\frac{\partial p}{\partial x}, \text{ for } R_0 \gg h_{bf} \tag{3}$$

3. Calculation

For understanding the flow behavior inside the filtration pore covering from the macroscale, multiscale to nanoscale, the following parameter is defined:

$$r_q = \frac{q_m}{q_{m,conv}} \tag{4}$$

The value of r_q can show how the flow in the pore deviates from the classical macroscopic flow theory when the size of the pore is changed from the macroscale to the nanoscale.

Substituting Eqs. (1) and (3) into Eq. (4) and re-arranging gives that:

$$\begin{aligned} r_q = 8(1-\frac{\lambda_x}{2})[\frac{\lambda_x^3}{2C_{y,1}}(1+\frac{1}{2\lambda_{bf,0}}-\frac{q_0-q_0^n}{q_0^{n-1}-q_0^n}\frac{\Delta_{n-2}}{h_{bf}})\frac{\varepsilon}{1+\frac{\Delta x}{D}} \\ -\frac{F_1\lambda_x^3}{12C_{y,1}}]C_{q,1}+\{1-\frac{16}{C_{y,1}}[\frac{F_2\lambda_{bf,0}^2}{6}-\frac{\lambda_{bf,0}}{1+\frac{\Delta x}{D}}(\frac{1}{2}+\lambda_{bf,0}- \\ \frac{(q_0-q_0^n)\Delta_{n-2}}{2(q_0^{n-1}-q_0^n)(R_0-h_{bf})})]\}\cdot(1-\lambda_x)^4, \text{ for } \lambda_x<1 \end{aligned} \tag{5}$$

where $C_{y,1}=\eta_{bf,1}^{eff}/\eta$ and $C_{q,1}=\rho_{bf,1}^{eff}/\rho$.

Substituting Eqs. (2) and (3) into Eq.(4) and re-arranging gives that:

$$r_q = -\frac{C_{q,2}(R_0)S(R_0)}{C_{y,2}(R_0)}, \text{ for } \lambda_x \geq 1 \tag{6}$$

where $C_{q,2}=\rho_{bf,2}^{eff}/\rho$ and $C_{y,2}=\eta_{bf,2}^{eff}/\eta$.

In the exemplary calculations, it was taken that $\Delta x/D = \Delta_{n-2}/D = 0.15$ and $\eta_{line,i}/\eta_{line,i+1} = q_0^m$, where q_0 and m are positive constant respectively (m is the index measuring the local viscosity inhomogeneity) (Jiang and Zhang 2022, Zhang 2014).

3.1 Parameter formulation

For the hydrophobic pore wall, the interaction between the pore wall and the flowing liquid is weak and the boundary layer is weakly adsorbed to the pore wall. However, for the hydrophilic pore wall, the liquid-pore wall interaction may be much stronger and it may be medium-level or even strong. The membrane polarity should significantly influence the liquid-pore wall interaction. The polar pore wall would have a relatively strong interaction with a polar liquid, while it would have a relatively weak interaction with a non-polar liquid. Normally, the non-polar pore wall has a relatively weak interaction with a non-polar liquid. The polarity or non-polarity of the pore wall can also be realized by coating a specific material on the pore wall. Besides these, both the temperature and pressure inside the pore will significantly influence the liquid-pore wall interaction; The higher temperature enlarges the distance between the molecule of the solid pore wall and the molecule of the flowing liquid, reduces the adsorption strength of the pore wall and weakens the liquid-pore wall interaction; While, the higher pressure has the opposite effect. In the present calculations, the weak, medium and strong liquid-pore wall interactions were considered respectively. The parameters in the above equations dependent on the liquid-pore wall interaction are formulated as follows respectively.

The parameter $C_{y,1}$ is expressed as (Zhang 2004, 2014):

$$C_{y,1}(H_{bf}) = \begin{cases} 1 & , \text{ for } H_{bf} \geq 1 \\ a_0 + \frac{a_1}{H_{bf}} + \frac{a_2}{H_{bf}^2} & , \text{ for } H_{bf} < 1 \end{cases} \tag{7}$$

where $H_{bf} = h_{bf}/h_{cr}$, h_{cr} is the critical thickness, and a_0, a_1 and a_2 are constant respectively. h_{cr} is the parameter characterizing the influence of the adsorbed layer thickness on the effective viscosity or average density of the adsorbed layer; Stronger the liquid-pore wall interaction, larger the value of h_{cr}, then greater the value of $C_{y,1}$ and more solidified the adsorbed layer (i.e. greater the value of $\eta_{bf,1}^{eff}$). This is based on the experimental observation that when the size of a nanochannel is critically large, the liquid confined in the nanochannel becomes continuum (Meyer *et al*. 1998).

The parameter $C_{q,1}$ is expressed as (Zhang 2004 and 2014):

$$C_{q,1}(H_{bf}) = \begin{cases} 1 & , \text{ for } H_{bf} \geq 1 \\ m_0 + m_1 H_{bf} + m_2 H_{bf}^2 + m_3 H_{bf}^3 & , \text{ for } H_{bf} < 1 \end{cases} \tag{8}$$

where m_0, m_1, m_2 and m_3 are constant respectively.

The parameter $C_{y,2}$ is expressed as (Zhang 2004, 2014):

$$C_{y,2}(\bar{R}_0) = \begin{cases} 1 & , \text{ for } \bar{R}_0 \geq 1 \\ a_0 + \frac{a_1}{\bar{R}_0} + \frac{a_2}{\bar{R}_0^2} & , \text{ for } \bar{R}_0 < 1 \end{cases} \tag{9}$$

where $\bar{R}_0 = R_0/R_{cr}$. R_{cr} is the critical radius for characterizing the influence of the pore radius on the effective viscosity and average density of the non-continuum film in the whole pore; $R_{cr} = 2h_{cr}$.

The parameter $C_{q,2}$ is expressed as (Zhang 2004, 2014):

Table 1(a) Liquid viscosity data for different liquid-pore wall interactions (Zhang 2004, 2014)

Interaction \ Parameter	a_0	a_1	a_2
Strong	1.8335	-1.4252	0.5917
Medium	1.0822	-0.1758	0.0936
Weak	0.9507	0.0492	1.6447×10^{-4}

Table 1(b) Liquid density data for different liquid-pore wall interactions (Zhang 2004, 2014)

Interaction \ Parameter	m_0	m_1	m_2	m_3
Strong	1.43	-1.723	2.641	-1.347
Medium	1.30	-1.065	1.336	-0.571
Weak	1.116	-0.328	0.253	-0.041

Table 1(c) Liquid non-continuum property data for different liquid-pore wall interactions (Zhang 2004, 2014)

Interaction \ Parameter	n_0	n_1	n_2	n_3
Strong	0.4	-1.374	-0.534	0.035
Medium	-0.649	-0.343	-0.665	0.035
Weak	-0.1	-0.892	-0.084	0.1

$$C_{q,2}(\bar{R}_0)=\begin{cases}1 & , \text{ for } \bar{R}_0\geq 1\\ m_0+m_1\bar{R}_0+m_2\bar{R}_0^2+m_3\bar{R}_0^3 & , \text{ for } \bar{R}_0<1\end{cases} \quad (10)$$

Eqs. (7)-(10) are the regressed equations for fitting the experimental data of the effective viscosity and average density of the confined liquid in the nanochannel which showed the dependence on the nanochannel size (Meyer *et al*. 1998, Zhang 2004).

The parameter *S* is expressed as (Zhang 2004, 2014):

$$S(\bar{R}_0)=\begin{cases}-1 & , \text{ for } \bar{R}_0\geq 1\\ [n_0+n_1(\bar{R}_0-n_3)^{n_2}]^{-1} & , \text{ for } n_3<\bar{R}_0<1\end{cases} \quad (11)$$

where m_2, m_3, n_2 and n_3 are constant respectively. Equation (11) is also the regressed equation for fitting the values of *S* obtained in MDS (Zhang 2016).

The parameters ε, F_1 and F_2 are expressed as respectively (Zhang 2020):

$$\varepsilon=4.56\times10^{-6}(\Delta_{n-2}/D+31.419)(n+133.8)(q_0+0.188)(m+41.62) \quad (12)$$

$$F_1=0.18(\Delta_{n-2}/D-1.905)(\ln n-7.897) \quad (13)$$

and

$$F_2=-3.707\times10^{-4}(\Delta_{n-2}/D-1.99)(n+64)(q_0+0.19)(m+42.43) \quad (14)$$

Eqs. (12)-(14) are the equations regressed out which well fit the actual calculated values of ε, F_1 and F_2. They have the merit of convenient calculation.

For the exemplary weak, medium and strong liquid-pore wall interactions considered, the parameter values are chosen as follows:

Weak interaction: m=0.5, n=3, $q_0=1.03$, h_{cr}=3.5nm

Medium interaction: m=1.0, n=5, $q_0=1.1$, h_{cr}=10nm

Strong interaction: m=1.5, n=8, $q_0=1.2$, h_{cr}=20nm

These parameter values fit the MDS results respectively for different levels of the liquid-channel wall interactions (Jiang and Zhang 2022, Zhang 2015, 2016).

The other input parameter values are shown in Tables 1(a)-1(c).

The parameter values in Tables 1(a)-1(c) for different liquid-pore wall interactions were chosen according to the rheological property measurements of the confined liquid in the nanochannel (Meyer *et al*. 1998) or the molecular dynamics simulation (MDS) results (Jiang and Zhang 2022, Zhang 2015 and 2016).

4. Results

Fig. 2 shows the variations of the value of r_q with h_{bf}/R_0 respectively for the weak, medium and strong liquid-pore wall interactions. It is shown that for $h_{bf}/R_0<0.01$, the value of r_q approaches to unity and the conventional hydrodynamic flow theory can be used to calculate the transferred mass through the pore; While for $h_{bf}/R_0>0.01$, the new calculation approach should be used by incorporating the adsorbed layer effect and the conventional calculation will overestimate the transferred mass owing to ignoring the adsorbed layer effect. For $0.01<h_{bf}/R_0<1$, the multiscale flow approach should be used for the calculation and it gives the mass flow rate through the pore significantly lower than the classical hydrodynamic theory calculation. Attend that for the multiscale flow with the value of h_{bf}/R_0 close to unity, the present multiscale calculation has pronounced errors, and the jump-up of all the three curves for the value of h_{bf}/R_0 around unity in Fig. 2 should be artificial and abandoned. For $h_{bf}/R_0>1$, the multiscale flow vanishes and the flow in the pore enters into the entire adsorbed layer flow regime; For this case, the nanoscale non-continuum flow approach should be used to make the calculation by incorporating both the non-continuum and rheological property variation effects of the layer.

Fig. 2 shows that for $h_{bf}/R_0>0.01$, the adsorbed layer has a significant influence on the flow in the pore, especially for $h_{bf}/R_0>1$ i.e., for the nanoscale non-continuum flow regime; With the increase of the interaction strength between the liquid and the pore, the mass flow rate through the pore is significantly reduced. It is shown that for $h_{bf}/R_0>1$, the medium and strong liquid-pore wall interactions both are very harmful for the mass transfer through the pore as the values of r_q are far lower than unity, and the weak liquid-pore wall interaction is mandatory for the good mass transfer or the high flux in the pore. Even for $0.01<h_{bf}/R_0<1$ i.e., the multiscale flow regime, the medium and strong liquid-pore wall interactions are also very harmful, and the weak liquid-pore wall interaction is plausible for the flux in the pore. Fig. 2

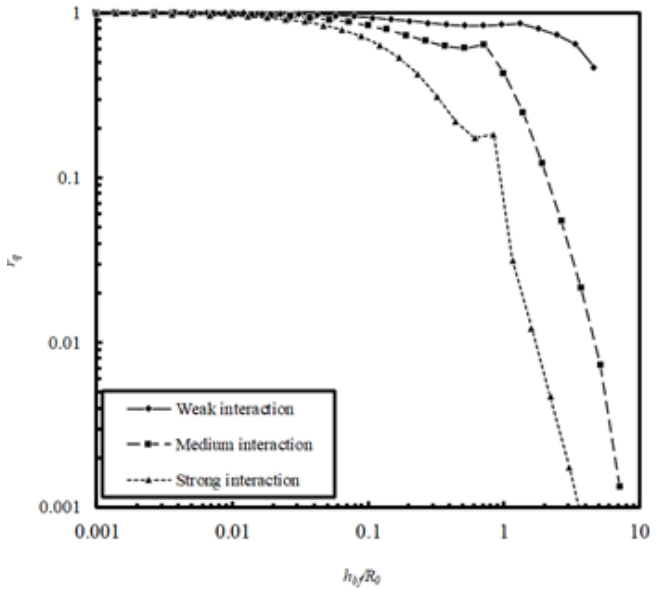

Fig. 2 The pore radius-dependent ratio r_q of the total mass flow rate through the filtration pore calculated from the multiscale or non-continuum nanoscale approaches to that calculated from the classical macroscopic flow theory

also shows that for $h_{bf}/R_0 > 0.01$, the value of r_q is rapidly reduced with the increase of h_{bf}/R_0, especially when $h_{bf}/R_0 > 1$. This obviously indicates that with the increase of h_{bf} or/and with the reduction of R_0, the flow rate through the pore is much faster reduced than the classical hydrodynamic theory prediction, owing to the multiscale flow effect or the nanoscale non-continuum flow effect. Fig. 2 suggests that with the increase of the membrane polarity, the transport of the polar liquid like water is more difficult through the pore with $h_{bf}/R_0 > 0.01$, particularly for smaller R_0 values, because of the increased liquid-pore wall interaction strength.

The results in Fig. 2 qualitatively agree with the molecular dynamics simulation results especially for $h_{bf}/R_0 > 1$ which show that the increase of the interaction strength between the channel wall and the liquid significantly reduces the mass flow rate through the nanochannel or the reduction of the channel size rapidly slows the liquid flow through the nanochannel if no wall slippage occurs (Liu and Li 2011, Takaba *et al*. 2007). Regarding the multiscale flow regime for $0.01 < h_{bf}/R_0 < 1$, the comparison of the present results with the experiments or the hybrid MDS-continuum fluid model needs to be done in the future.

5. Conclusions

The analytical results are presented for the mass flow rate through a cylindrical filtration pore in micro/nano porous filtration membranes covering from the macroscale, multiscale to nanoscale. Owing to the effect of the adsorbed layer on the pore wall, when the radius R_0 of the filtration pore is less than one hundred times of the thickness h_{bf} of the adsorbed layer, the classical hydrodynamic flow analysis is inaccurate and the corresponding analysis should incorporate the adsorbed layer effect. For $0.01 < h_{bf}/R_0 < 1$, the multiscale analysis should be required owing to the simultaneous occurring of the adsorbed layer flow and the continuum liquid flow. For $h_{bf}/R_0 > 1$, the non-continuum nanoscale analysis should be required owing to the entire adsorbed layer flow in the pore. However, for $h_{bf}/R_0 < 0.01$, the continuum hydrodynamic flow analysis should still be valid owing to the negligible effect of the adsorbed layer.

The calculation results show that whenever in the multiscale flow or in the non-continuum nanoscale flow, the adsorbed layer has a significant influence on the flow in the pore. The medium and strong liquid-pore wall interactions are very harmful for the flux in the nanoscale pore because of the adsorbed layer effect, and the weak liquid-pore wall interaction is very beneficial for the high flux in the pore. Also, the reduction of the radius of the pore much more rapidly drops the flow rate through the pore than the classical hydrodynamic flow theory prediction owing to the significant adsorbed layer effect when the multiscale flow or the non-continuum nanoscale flow occur.

References

Ariono, D., Aryanti, P.T.P., Wardani, A.K. and Wenten, I.G. (2018), "Fouling characteristics of humic substances on tight polysulfone-based ultrafiltration membrane", *Membr. Water Treat.*, **9**(5), 353-361. https://doi.org/10.12989/mwt.2018.9.5.353.

Atkas, O. and Aluru, N.R. (2002), "A combined continuum/ DSMC technique for multiscale analysis of microfluidic filters", *J. Comput. Phys.*, **178**(2), 342-372. https://doi.org/10.1006/jcph.2002.7030.

Baker, L.A. and Bird, S.P. (2008), "Nanopores: A makeover for membranes", *Nature Nanotech.*, **3**, 73-74. https://doi.org/10.1038/nnano.2008.13.

Borg, M.K., Lockerby, D.A. and Reese J. M. (2013), "A multiscale method for micro/nano flows of high aspect ratio", *J. Comput. Phys.*, **233**, 400-413. https://doi.org/10.1016/j.jcp.2012.09.009.

Borg, M.K., Lockerby, D.A., Ritos, K. and Reese, J.M. (2018), "Multiscale simulation of water flow through laboratory-scale nanotube membranes", *J. Membr. Sci.*, **567**, 115-126. https://doi.org/10.1016/j.memsci.2018.08.049.

Bottino, A., Capannelli, G., Comite, A., Ferrari, F. and Firpo, R. (2011), "Water purification from pesticides by spiral wound nanofiltration membrane", *Membr. Water Treat.*, **2**(1), 63-74. http://doi.org/10.12989/mwt.2011.2.1.063.

Brown, C.E., Everett, D.H., Powell, A.V. and Thome, P.E. (1975), "Adsorption and structuring phenomena at the solid/liquid interface", *Faraday Discus. Chem. Soc.*, **59**, 97-108. https://doi.org/10.1039/DC9755900097.

Elizabeth, E.M.O., Barbosa, C.C.R. and Afonso, J.C. (2012), "Selectivity and structural integrity of a nanofiltration membrane for treatment of liquid waste containing uranium", *Membr. Water Treat.*, **3**(4), 231-242. http://dx.doi.org/10.12989/mwt.2012.3.4.231.

El-ghzizel,S., Jalté, H., Zeggar, H., Zait, M., Belhamidi, S., Tiyal, F., Hafsi, M., Taky, M. and Elmidaoui, A.(2019), "Autopsy of

nanofiltration membrane of a decentralized demineralization plant", *Membr. Water Treat.*, **10**(4), 277-286. https://doi.org/0.12989/mwt.2019.10.4.277.

Fissel, W.H., Dubnisheva, A., Eldridge, A.N., Fleischman, A.J., Zydney, A.L. and Roy, S. (2009), "High-performance silicon nanopore hemofiltration membranes", *J. Membr. Sci.*, **326**(1), 58- 63. http://doi.org/10.1016/j.memsci.2008.09.039.

Jackson, E.A. and Hillmyer, M.A. (2010), "Nanoporous membranes derived from block copolymers: From drug delivery to water filtration", *ACS Nano*, **4**(7), 3548-3553. http://doi.org/10.1021/nn1014006.

Jiang, C.T. and Zhang, Y.B. (2022), "Direct matching between the flow factor approach model and molecular dynamics simulation for nanochannel flows", *Sci. Rep.*, **12**(1), 396. https://doi.org/10.1038/s41598-021-04391-5.

Jin, Y., Choi, Y., Song, K.G., Kim, S. and Park, C. (2019), "Iron and manganese removal in direct anoxic nanofiltration for indirect potable reuse", *Membr. Water Treat.*, **10**(4), 299-305. https://doi.org/0.12989/mwt.2019.10.4.299.

Khalili-Araghi, F., Gumbart, J., Wen, P., Sotomayor, M., Tajkhorshid, E. and Schulten, K. (2009), "Molecular dynamics simulations of membrane channels and transporters", *Curr. Pin. Struct. Biol.*, **19**(2), 128-137. https://doi.org/10.1016/j.sbi.2009.02.011.

Liu, C. and Li, Z. (2011), "On the validity of the Navier-Stokes equations for nanoscale liquid flows: The role of channel size", *AIP Adv.*, **1**(3), 032108. https://doi.org/10.1063/1.3621858.

Meyer, E., Overney, R.M., Dransfeld, K. and Gyalog, T. (1998), *Friction and Rheology on the Nanometer Scale*, World Scientific Press, New Jersey, U.S.A.

Sanjay, R., Nagarajan, P., Sabyasachi, G., Subhadip, M., Suryasarathi, B. and Narayan, C.D. (2021), "Porous graphene-based membranes: Preparation and properties of a unique two-dimensional nanomaterial membrane for water purification", *Sep. Purif. Rev.*, **50**(3), 262-282. https://doi.org/10.1080/15422119.2020.1725048.

Sommerer, T.J. and Kushner, M.J. (1992), "Numerical investigation of the kinetics and chemistry of rf glow discharge plasmas sustained in He, N_2, O_2, He/N_2/O_2, He/CF_4/O_2, and SiH_4/NH_3 using a Monte Carlo-fluid hybrid model", *J. Appl. Phys.*, **71**(4), 1654-1673. https://doi.org/10.1063/1.351196.

Surwade, S.P., Smirnov, S.N., Vlassiouk, I.V., Unocic, R.R., Veith, G.M., Dai, S. and Mahurin, S.M. (2015), "Water desalination using nanoporous single-layer grapheme", *Nature Nanotech.*, **10**(5), 459-464. https://doi.org/10.1038/nnano.2015.37.

Takaba, H., Onumata, Y. and Nakao, S. (2007), "Molecular simulation of pressure-driven fluid flow in nanoporous membranes", *J. Chem. Phys.*, **127**(5), 054703. https://doi.org/10.1063/1.2749236.

Wang, J.B., Cheng, J.Y., Qing, Shi, T., Huang, Q. and He, X.W. (2013), "Membrane fouling mechanism and its control in the treatment of brackish water with reverse osmosis process", *Adv. Mater. Res.*, **788**, 268-274. https://doi.org/10.4028/www.scientific.net/amr.788.268.

Yang, J.M., Jia, R.B., Wang, Z.J., Yang, X.L. and Pan, Z.B. (2012), "Study on production wastewater in water treatment plants by Submerged micro-filtration membrane", *Adv. Mater. Res.*, **374-377**, 982-986. https://doi.org/10.4028/www.scientific.net/amr.374-377.982.

Yoon, S.H. (2018), "Direct membrane filtration of wastewater under very short hydraulic retention time", *Adv. Environ. Res.*, **7**(7), 39-52. http://doi.org/10.12989/aer.2018.7.1.039.

Zhang, Y.B. (2004), "Modeling of molecularly thin film elastohydrodynamic lubrication", *J. Balkan Trib. Assoc.*, **10**, 394-421.

Zhang, Y.B. (2014), "Lubrication analysis for a line contact covering from boundary lubrication to hydrodynamic lubrication: Part I- Micro contact results", *J. Comput. Theor. Nanosci.*, **11**(1), 62-70. https://doi.org/10.1166/jctn.2014.3318.

Zhang, Y.B. (2015), "The flow factor approach model for the fluid flow in a nano channel", *Int. J. Heat Mass Transf.*, **89**, 733-742. https://doi.org/10.1016/j.ijheatmasstransfer.2015.05.092.

Zhang, Y.B. (2016), "The flow equation for a nanoscale fluid flow", *Int. J. Heat Mass Transf.*, **92**, 1004-1008. https://doi.org/10.1016/j.ijheatmasstransfer.2015.09.008.

Zhang, Y.B. (2017), "Transport in nanotube tree", *Int. J. Heat Mass Transf.*, **114**, 536-540. https://doi.org/10.1016/j.ijheatmasstransfer.2017.06.105.

Zhang, Y.B. (2020), "Modeling of flow in a very small surface separation", *Appl. Math. Mod.*, **82**, 573-586. https://doi.org/10.1016/j.apm.2020.01.069.

Zhang, Y.B. (2021), "Modeling of flow in a micro cylindrical tube with the adsorbed layer effect: Part I-Results for no interfacial slippage", *Int. J Heat Mass Transf.*, submitted.

CC